03,06,09,10

Processes of a charge delocalization in monocrystal $TlGaSe_2$: Nd and defreezing of electrets states

© A.P. Odrinskii

Institute of Technical Acoustics, National Academy of Sciences of Belarus,
Vitebsk, Belarus

E-mail: a.odrinsky@gmail.com

Received October 24, 2023
Revised October 24, 2023
Accepted October 25, 2023

Eight processes of charge delocalization have been observed in $TlGaSe_2$ crystal doped by neodymium impurities by the photoinduced current transient spectroscopy. The processes associated with intrinsic defects of crystal and introduced impurity atoms have been identified. The modification of processes of charge thermal emission was found that was caused by formation of electrets states in crystal. The process of charge delocalization in the region of defreezing temperature of electrets states is considered. Displacement of Arrenius plot for the given process in neodymium-doped crystal concerning undoped one is interpreted as amplification of thermal emission of charge in undoped crystal due to phonon-assistant tunneling.

Keywords: ferroelectric semiconductors, charge localization centers, electret states, thermal emission enhancement.

DOI: 10.61011/PSS.2024.01.57849.238

1. Introduction

2D-structured single-crystals of ferroelectric semiconductor $TlGaSe_2$ have drawn the interest of researchers over a number of years. With significant anisotropy, they have a set of unique physical properties that have good prospects of application in optoelectronics [1,2], construction of various infrared and visible range sensors [3,4], X-ray and gamma radiation sensors [5], as memory elements [6,7], etc. $TlGaSe_2$ is offered as a prototype of a brand-new ferroelectric photovoltaic solar converter [8]. Having the known memory effects [9], tendency to form heterogeneity of electrical [8,10] and optical properties [11] not limited by a ferroelectric state temperature range, the crystal complex enough object of research [12]. Investigation of the charge carrier localization and delocalization processes on crystalline structure defects, including intentionally introduced impurity atoms, is of key interest in understanding of the electrical properties of $TlGaSe_2$. It is, first of all, due to the fact that defects are capable of participating in formation of heterogeneity of a crystal charge pattern by playing a role of charge carrier localization centers (CLC). Currently, crystalline structure defects in $TlGaSe_2$ are understudied. This relates both to the identification of their origin and to an equally important question [13] — understanding their role and mechanisms of interaction with other electrical activity of the crystal that is not formally associated with CLC: crystal polarization, photovoltaic currents, including photogalvanic current.

Investigation of charge delocalization in neodymium-doped $TlGaSe_2$ crystal by the photoinduced current transient spectroscopy (PICTS) method is described herein [14]). Non-equilibrium filling of CLC by means of crystal photoexcitation that is used in the photoinduced current transient spectroscopy provides a unique opportunity of detailed study of the electrical activity of defects in presence of other electrical activity of crystal with the involvement of data interpretation techniques used in the deep level transient spectroscopy (DLTS) proven in the semiconductor materials science for electronics applications.

2. Sample and measurement procedure

$TlGaSe_2$ crystal is neodymium- doped with concentration 0.1 at.%. The sample had dimensions of $5.5 \times 3.8 \times 0.4$ mm and *p*-type conductivity with the charge carrier concentration of $\sim 3 \cdot 10^{13}$ cm^{-3} at 300 K. Ohmic contacts were made using silver paste on the sample end surfaces with partial coverage of the frontal surface — cleavage plane. Current flow geometry — along the crystal layers. Light excitation fell perpendicularly to the crystal surface — cleavage plane. More detailed data on a set of CLC according to the approach in [15] was obtained using the crystal excitation with different photon energies $h\nu = 1.12-2.0$ eV at the photon flux density on the sample surface $\sim 10^{15}$ cm$^{-2} \cdot$ s^{-1}. The measuring system and measurement procedure were the same as described in [16]. The sample excitation frequency was chosen from 25–50 Hz with a light pulse width of $\sim 3-6$ ms. Photoresponse relaxation was recorded during sample heating at a rate of ~ 2 K/min within the temperature range 78–330 K at 1 K intervals. Recording included point-by-point accumulation and averaging of the signal kinetics (64 instances) containing 2000 sampling spaced at fixed time intervals.

3. Results and discussion

Figure 1 shows the variations with the crystal photoresponse amplitude temperature. The curves are numbered according to the testing sequence, including recording of data sets regarding the crystal photoresponse kinetics variation with temperature. First of all, a recurring pattern of dependences obtained in the identical photoexcitation conditions shall be noted — curves *1* and *4*. Curves *5* and *6* plotted using the sets of data successively recorded with a relatively small difference in the light excitation photon energies also differ considerably in a low-temperature range of $T < 200$ K, while at a higher temperature they almost coincide. In this region, they are little different from dependence *7* obtained in excitation with $h\nu \approx E_g$, where E_g is the band gap. Here, in the data sets corresponding to curves $5-7$, abnormal photoresponse relaxation kinetics in the temperature range of $225-260$ K are observed. Examples of the observed anomalies are shown in Figure 2.

With increasing $h\nu$ of the photoexcitation, anomalies of this kind, but considerably more intensive, are also typical for undoped $TlGaSe_2$ crystal [17]. The neodymium-doped sample shows photoresponse relaxation anomalies also in the data set recorded at the lowest photon energy, but directly after the experiment with excitation $h\nu \approx E_g$, which agrees completely with the memory effects known for $TlGaSe_2$ [9,18], as well as with formation of electrical inhomogeneity of the crystal [8].

Figure 3 shows the examples of PICTS- spectra measured on $TlGaSe_2:Nd$ crystal. Straight lines show the displacement of the peak temperature position in the set of spectra that are different in the characteristic relaxation times — τ_i, where i is the spectrum number. This displacement is activated with the temperature of charge delocalization with CLC. In the crystal spectra, eight processes denoted in the Figure as $N1-N8$ may be reliably identified. In Figure 3, *a*, peak $N8$ within the range of $T > 270$ K has the dominating position, which suggests high intensity of the process and implies considerable concentration of the corresponding CLC [19]. Dominating position of peak $N8$ is observed in the spectra with high characteristic relaxation times. With decreasing τ_i, the peak height $N8$ becomes comparable with $N7$, and then $N7$ is dominating. The same trend is also observed in the spectrum set shown in Figure 3, *b*, obtained during excitation with higher photon energies $h\nu = 1.68$ eV. With further increase in the light excitation photon energy ($h\nu \geq 1.8$ eV), the dominating position in the spectra of peak $N7$ with decreasing τ_i is expressed more distinctly (see Figure 3, *c*), while the contribution of $N8$ is hardly identified. Such feature of spectra, i.e. the growth of peak $N7$ compared with other peaks, is observed for all data sets containing distinctive anomalies in the relaxation kinetics.

Figure 4 shows the dependence of the charge delocalozation rate on the temperature for the processes detected on $TlGaSe_2:Nd$ crystal. The Table shows the delocalization

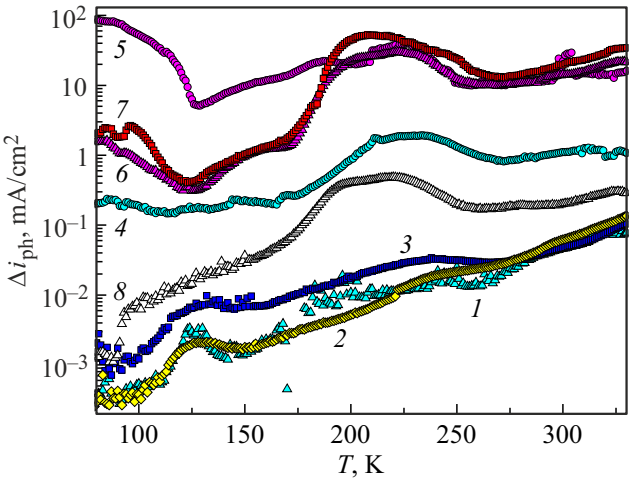

Figure 1. Temperature dependence of the photocurrent density. Curves *1*–*8* were obtained at the excitation with $h\nu = 1.68$, 1.37, 1.23, 1.68, 1.88, 1.81, 2.00 and 1.12 eV, respectively. The curves are numbered according to the recording sequence, corrected to the equal photon flux taking into account DKSSh-500 spectrum.

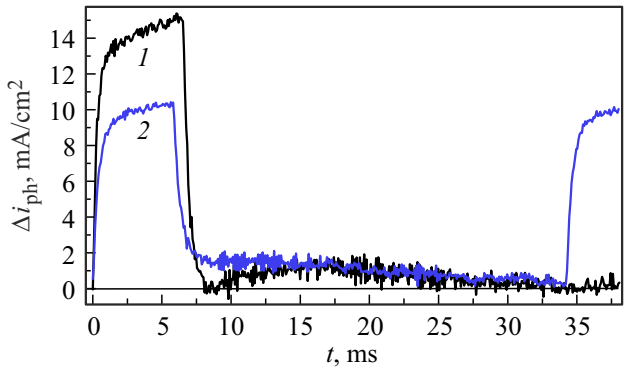

Figure 2. Crystal photoresponse kinetics at 257 K under the excitation with $h\nu = 2.0$ eV — curve *1* and $h\nu = 1.88$ eV — curve *2*.

recording temperature ranges — $\Delta_0 T$ together with the corresponding CLC parameters measured using the standard DLTS analysis technique: E_t is the delocalization thermal activation energy and σ_t is the effective capture cross-section.

The Arrhenius plot position of process $N1$ in Figure 4 may be compared with the thermal emission with CLC $A1$ [16,20] observed before in the temperature range of the phase transition from the commensurate ferroelectric phase to the incommensurate phase, $T = 107$ K [10]. $N2$ may be also identified with $A2$ process described in [16,20] that flows in the temperature range of the phase transition from the incommensurate ferroelectric phase to paraelectric phase $T = 120$ K [10]. The Arrhenius plot for processes $N3$ and $N5$ is adequately comparable with $A3$ and $A4$ processes observed before [16]. This allows to identify CLC that are responsible for these processes as

intrinsic defects of the crystal. On the other hand, it can be assumed that $N4$ and $N6$, for which the Arrhenius line is much different from the processes in an undoped crystal, are caused by delocalization from centers associated with introduction of the neodymium impurity.

For intensive process $N7$, the Arrhenius line is also much different from the processes observed in the undoped crystal [16,20], however, its interpretation as a process associated with impurity atoms rises doubts, which is discussed in the next section.

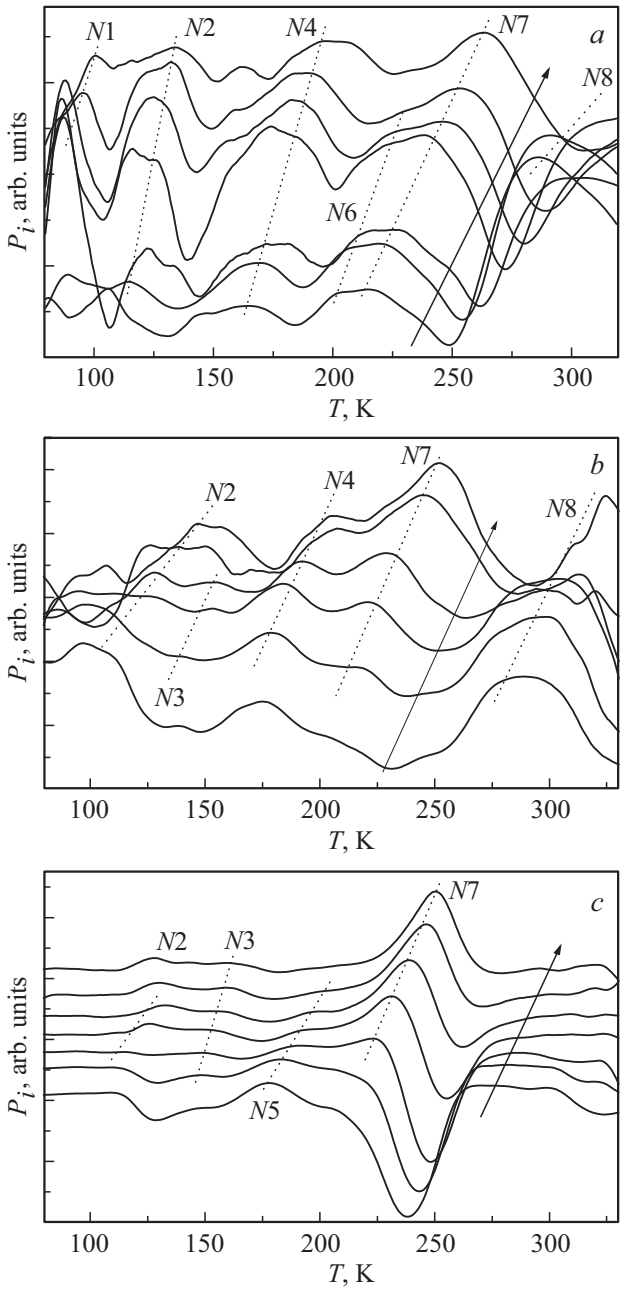

Figure 3. PICTS-spectra sets recorded on $TlGaSe_2$: Nd crystal at the excitation with *a*) $h\nu = 1.37$ eV; *b*) $h\nu = 1.68$ eV; *c*) $h\nu = 1.88$ eV. The arrow shows the characteristic spectrum relaxation time sequence:*a*) 33.9, 20.1, 9.88, 3.23, 1.59, 0.82 and 0.35 ms; *b*) 33.9, 20.1, 11.9, 4.76, 1.18 and 0.66 ms; *c*) 31.4, 18.1, 9.88, 4.76, 2.46, 1.18 and 0.61 ms. The spectra are adjusted by the dominating peak height and successively displaced on the *y* axis.

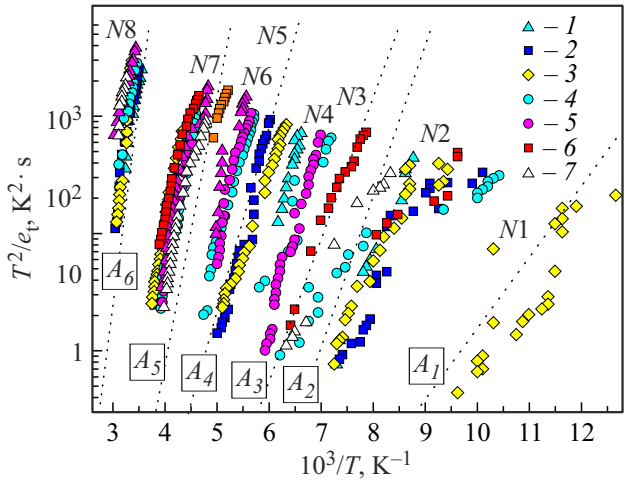

Figure 4. Dependence of the charge delocalization with CLC in $TlGaSe_2$: Nd crystal from the temperature. Data numbering — as shown in Figure 1. Delocalization processes $A1-A6$ in an undoped crystal according to [16] are shown by the dotted lines.

CLC parameters

Process	$\Delta_0 T$, K	E_t, eV	σ_t, cm^2
$N1$	79–104	0.12	$2.8 \cdot 10^{-16}$
$N2$	108–138	0.15	$1.1 \cdot 10^{-16}$
$N3$	127–156	0.22	$1.4 \cdot 10^{-15}$
$N4$	143–169	0.39	$1.4 \cdot 10^{-12}$
$N5$	166–200	0.37	$8.8 \cdot 10^{-13}$
$N6$	192–203	0.32	$4.9 \cdot 10^{-15}$
$N7$	218–256	0.44	$6.4 \cdot 10^{-14}$
$N8$	286–329	0.54	$4.7 \cdot 10^{-15}$

3.1. Discussion of the identification of process $N7$

For process $N7$, charge delocalization recording region $\Delta_0 T$ actually coincides with the region where photoresponse relaxation anomaly of our sample is observed. This region in undoped $TlGaSe_2$ showed change of the mechanism responsible for abnormal crystal response to light [17]: at a temperature below ~ 235 K, response caused by the electretic states formed in the low-temperature ferroelectric phase is dominating while at a higher temperature, photovoltaic emf action prevails. Thus, this charge delocalization process may be treated as unfreezing of electretic states by comparing with the typical intrinsic defect $TlGaSe_2$ that contributes to formation of the electretic crystal states.

High intensity of processes $N7$ and $N8$ is indicative of considerable concentration of appropriate CLC and, therefore, of the capability of these processes to have a significant effect on the electrical properties of a whole crystal. Peak $N8$ is in the spectra recorded with the photon

excitation $h\nu < 1.8$ eV and is not observed in spectra recorded with the excitation that provokes anomalies in the relaxation (at $h\nu \geq 1.8$ eV). And this agrees completely with the electrical inhomogeneity of the test sample when, during relaxation, the thermal emission of a localized charge is accompanied by spatial movement of free charge carriers in the internal field of the crystal. In this view, contribution of processes $N1-N5$ to the photoresponse relaxation recorded not in all conducted tests is also consistent with the electrical inhomogeneity of the sample. High intensity of process $N7$ is observed not in all tests, which is also consistent with the electrical inhomogeneity of the crystal. However, it is consistently recorded irrespective of the chosen excitation $h\nu$, which is more comparable with the assumption that $N7$ is a typical center for $TlGaSe_2$ than CLC attributed to the introduced impurity atoms.

During the excitation that provokes photoresponse anomalies ($h\nu \geq 1.8$ eV), relaxation anomalies are observed on $TlGaSe_2:Nd$ that are considerably weaker than those in the undoped crystal. Investigation of photoexcitation response evolution with $h\nu \geq E_g$ in the isothermal mode using the techniques from [8] has confirmed significant decrease of the effects associated with the photogalvanic emf acting in the neodymium-doped sample. At the same time, the excitation with $h\nu \geq 1.8$ eV leads to a characteristic kind of spectra shown in Figure 3, *c*.

Figure 5 shows the analysis of peak height variation in the set of spectra according technique [21]. For process $N7$, variations of diagram $[W_i/P_i, e_{ti}]$ are apparent, where W_i, P_i and e_{ti} are the characteristic coefficient, peak height and characteristic thermal emission rate of the i-th spectrum. However, for the data acquired in the excitation mode that provokes crystal response anomalies, dependences are linear, which is typical for photocurrent relaxation that is defined exclusively by recombination of non-equilibrium free charge carriers [21]: $P_i/W_i \propto n_{t0} = N_t/(1+\beta)$, where N_t is the CLC concentration, n_{t0} is the concentration of non-equilibriously filled CLC, β is the ratio of CLC filling and emptying rates. At the same time, for other processes with the excitation $h\nu \geq 1.8$ eV, diagram $[W_i/P_i, e_{ti}]$ is exclusively superlinear as shown in Figure 5, *b* and *c*. This indicates that the contribution of all delocalization processes to the crystal photoresponse relaxation, except for process $N7$, is modified. This explains the typical view of spectra in Figure 3, *c*. Such type of diagram (overestimation of the contribution at low characteristic relaxation times — τ_i and suppression of the contribution at high τ_i values) has been observed before on an electrically inhomogeneous $TlGaSe_2$ crystal [22]. It occurs as a result of additional contribution to the relaxation of diffusion current signal of photoinjected carriers rom high-resistance regions of the crystal. The absence of modification for $N7$ agrees completely with a special role of this process, its interpretation as electret defrosting and interpretation of the corresponding CLC as making an important contribution to the formation of electretic states of the crystal.

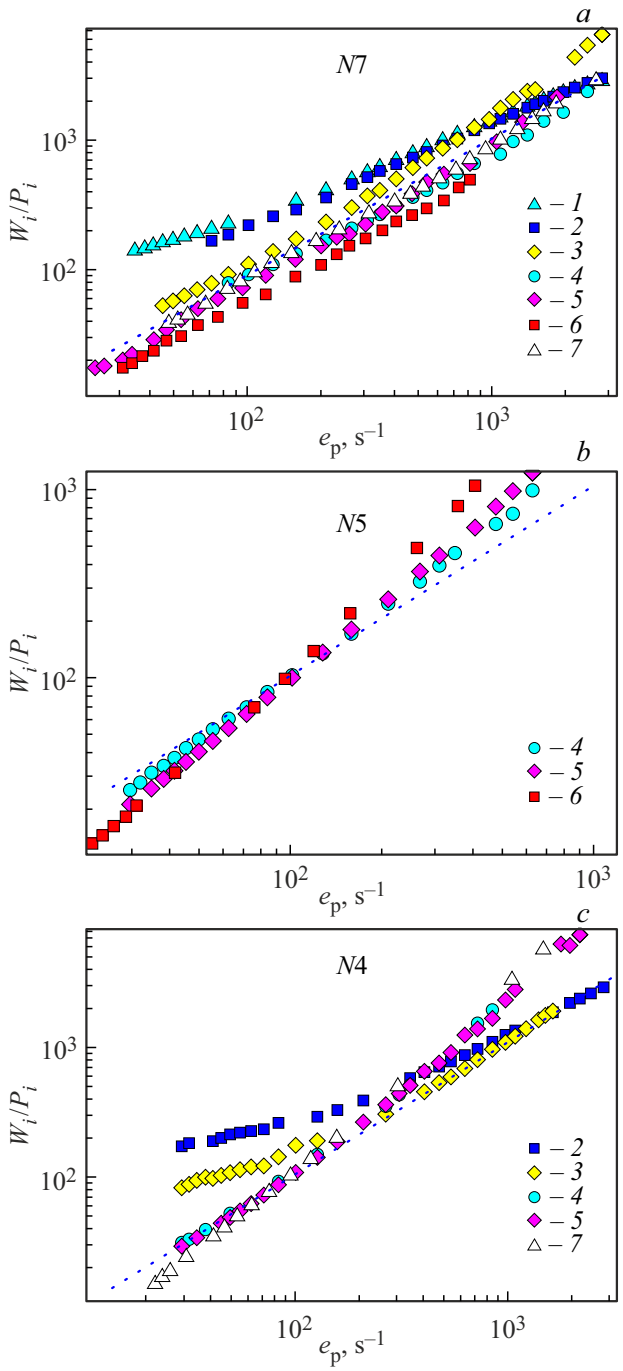

Figure 5. Dependence of peak height P_i on the charge delocalization rate e_p for processes *a*) $N7$, *b*) $N5$ and *c*) $N4$. The curves are numbered as shown in Figure 1.

The typical view of spectra (see Figure 3, *c*) was also observed on other rare-earth-doped (Er, Tb) samples and on the undoped $TlGaSe_2$ sample in the mode of injection from contact and with the excitation with $h\nu \geq 1.8$ eV. Figure 6 shows comparison of the Arrhenius plot of process $N7$ with these data. It is apparent that dependences *2–7* comply with the data for $TlGaSe_2:Tb$ (dependence *8*) and for the undoped crystal (dependence *9*).

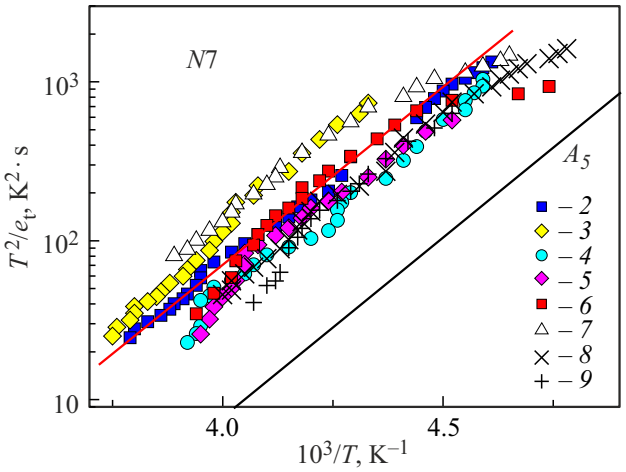

Figure 6. Variation of the delocalization temperature rate of process $N7$ in crystal $TlGaSe_2:Nd$ — dependences $2-7$ (numbered as shown in Figure 1), $TlGaSe_2:Tb$ — dependence *8*. Dependence *9* was obtained on the undoped crystal in the contact injection mode. The dotted line shows process $A5$ according to [16].

Thus, this strongly suggests that the charge delocalization process recorded in the temperature range of $T \approx 220-260$ K is caused by CLC typical for $TlGaSe_2$ that makes a strong contribution to formation of electretic crystal states, and $N7$ shall be compared with CLC $A5$ [16]. However, assuming this, quite considerable displacement of the Arrhenius line equal to ~ 20 K shall be explained. This displacement shall be interpreted in terms of charge thermal emission enhancement in the undoped crystal.

3.2. Thermal emission enhancement effect

The effect of the electric field on the charge delocalization process is estimated below [23]. It is known that, due to the Pool–Frenkel effect [24], application of an external electric field with strength E results in the enhancement of thermal emission $e(E)/e(0) \propto \exp(E_{PF}/k_BT)$, where $e(E)$ and $e(0)$ are charge delocalization rates with and without the electric filed, respectively, k_B is the Boltzmann constant, T is the temperature. The Pool–Frenkel energy $E_{PF} = 2(ze^3E/\varepsilon)^{1/2}$, where z is the CLC charge state, e is the elementary charge, ε is the dielectric constant. Then the presence of the internal electric field in the crystal resulting in the intensification of the charge delocalization process can explain the Arrhenius line displacement on the temperature scale. The displacement may be assessed as: $\Delta T \approx -E_{PF}T_0/E_t$, where E_t is the energy of CLC charge delocalization activation, T_0 is the temperature at which the defined delocalization rate is observed without the electric field. Assuming the relative dielectric constant as~ 5 [25], $z = 1$, field strength as 200 V/cm, we will obtain $E_{PF} \approx 17$ meV at $T_0 \approx 250$ K which makes the thermal emission 2.2 times higher and provides the displacement estimate as $\Delta T \approx 10.6$ K. Thus, the estimated enhancement of the thermal emission of process $N7$ due to the Pool–Frenkel effect does not explain the temperature shift of the Arrhenius plot. On the other hand, much stronger dependence of the thermal emission enhancement on the field strength for the phonon-assisted tunneling effect [23] can explain the temperature shift of the Arrhenius plot. This assumption agrees well with the known observations of the memory effects for the acoustic emission in this temperature range [26].

4. Conclusion

On the neodymium-doped crystal, charge delocalization processes, that had not been observed earlier, were found in the temperature ranges 143–169 and 192–203 K and were probably associated with the introduced impurity atoms. It may be concluded that introduction of neodymium in the crystal results in formation of CLC that are responsible for these processes that represent either an impurity atom introduction defect or a substitution defect or a more complex impurity-atom-assisted defect.

It has been found that neodymium-doping of the crystal results in weakening of effects associated with photogalvanic emf action in the crystal.

It is shown that the charge delocalization process in the temperature range $T \approx 220-260$ K is attributed to charge localization centers typical for the crystal that make a strong contribution to the formation of electretic crystal states. Displacement of the Arrhenius plot for this process relative to the data recorded on undoped $TlGaSe_2$ crystal is interpreted as the thermal emission enhancement on the undoped crystal due to the phonon-assisted tunneling effect.

Funding

The study was funded by the Belarusian Republican Foundation for Fundamental Research (grant No. F22-127).

Conflict of interest

The author declares that he has no conflict of interest.

References

[1] A. Qasrawi, A. Omar, A.M. Azamtta, N.M. Gasanly. Phys. Status Solidi A **212**, *3*, 600 (2015).
[2] V. Grivickas, V. Bikbajevas, K. Gulbinas, V. Gavryushin, J. Linnros. Phys. Status Solidi B **244**, *12*, 4624 (2007).
[3] S. Yang, M. Wu, H. Wang, H. Cai, L. Huang, C. Jiang, S. Tongay. 2D Mater. **4**, *3*, 035021 (2017).
[4] V. Grivickas, K. Gulbinas, V. Gavryushin, V. Bikbajevas, O.V. Korolik, A.V. Mazanik, A.K. Fedotov. Phys. Status Solidi RRL **8**, *7*, 639 (2014).
[5] S. Johnsen, Z. Liu, J.A. Peters, J.-H. Song, S. Nguyen, C.D. Malliakas, H. Jin, A.J. Freeman, B.W. Wessels, M.G. Kanatzidis. J. Am. Chem. Soc. **133**, *26*, 10030 (2011).

[6] M.-H.Yu. Seyidov, R.A. Suleymanov, E. Balaban, Y. Sale. J. Appl. Phys. **105**, *15*, 152106 (2014).
[7] B.B. Kandemir, S. Gören, M. Erdem, A. Cengiz, Y. Şale, A.K. Fedotov, T.G. Mammadov, M.-H.Yu. Seyidov. Semicond. Sci. Technol. **35**, *12*, 125010 (2020).
[8] A.P. Odrinskii. Phys. Solid State **63**, *8*, 1288 (2021).
[9] M.-H.Yu. Seyidov, R.A. Suleymanov, E. Balaban, Y. Sale. Ferroelectrics **481**, *1*, 77 (2015).
[10] V. Grivickas, A. Odrinski, V. Bikbajevas, K. Gulbinas. Phys. Status Solidi B **250**, *1*, 160 (2013).
[11] N. Mamedov, Y. Shim, N. Yamamoto. Jpn. J. Appl. Phys. **41**, *11S*, 7254 (2002).
[12] A.M. Panich. J. Phys.: Condens. Matter **20**, *29*, 293202 (2008).
[13] E.R. Weber. Physica B **340**–**342**, 1 (2003).
[14] C. Hurter, M. Boilou, A. Mitonneau, D. Bois. Appl. Phys. Lett. **32**, *12*, 821 (1978).
[15] K. Ikeda, Y. Ishii. Jpn. J. Appl. Phys. **26**, *3R*, 377 (1987).
[16] M.H.Y. Seyidov, F.A. Mikailzade, T. Uzun, A.P. Odrinsky, E. Yakar, V.B. Aliyeva, S.S. Babayev, T.G. Mammadov. Physica B **483**, 82 (2016).
[17] A.P. Odrinskii, M.-H.Yu. Seyidov, T.G. Mammadov, V.B. Alieva. Phys. Solid State **59**, *3*, 457 (2017).
[18] M.-H.Yu. Seyidov, R.A. Suleymanov, E. Balaban, Y. Sale. J. Appl. Phys. **114**, *9*, 093706 (2013).
[19] A.P. Odrinskii. Semicond. **39**, *6*, 629 (2005).
[20] A.P. Odrinskii. Phys. Solid State **56**, *2*, 335 (2014).
[21] A.P. Odrinskii, T.G. Mammadov, M.-H.Yu. Seyidov, V.B. Alieva. Phys. Solid State **56**, *8*, 1605 (2014).
[22] A.P. Odrinskii. Phys. Solid State **62**, *4*, 682 (2020).
[23] S.D. Ganichev, E. Ziemann, W. Prettl, I.N. Yassievich, A.A. Istratov, E.R. Weber. Phys. Rev. B **61**, *15*, 10361 (2000).
[24] J. Frenkel. Phys. Rev. **54**, *8*, 647 (1938).
[25] F. Salehli, Y. Bakış, M.-H.Yu. Seyidov, R.A. Suleymanov. Semicond. Sci. Technol. **22**, *8*, 843 (2007).
[26] Yu.P Gololobov, V.M. Perga, I.N. Salivonov, E.E. Shchigol. FTT **34**, *1*, 115 (1992). (in Russian).

Translated by E.Ilinskaya